Faraday Discussions

Cite this: *Faraday Discuss.*, 2014, **170**, 203

PAPER

# Quantitative *in situ* and real-time monitoring of mechanochemical reactions

Ivan Halasz,*[a] Tomislav Friščić,*[b] Simon A. J. Kimber,[c] Krunoslav Užarević,[a] Andreas Puškarić,[a] Cristina Mottillo,[b] Patrick Julien,[b] Vjekoslav Štrukil,[ab] Veijo Honkimäki[c] and Robert E. Dinnebier[d]

Received 16th February 2014, Accepted 19th February 2014
DOI: 10.1039/c4fd00013g

An experimental technique for *in situ* and real-time monitoring of mechanochemical reactions in a shaker ball mill was recently described, which utilises highly penetrating X-ray radiation available at the ID15B beamline of the European Synchrotron Radiation Facility. Herein, we describe the first attempts to perform such reaction monitoring in a quantitative fashion, by introducing an internal X-ray diffraction standard. The use of silicon as an internal standard resolved the issue with variations of the amount of the sample in the X-ray beam due to the non-uniform distribution of the sample in the reaction jar and allowed, *via* Rietveld analysis, the first quantitative estimate of the amorphous phase content in a mechanochemical reaction as it is being milled. We also highlight problems associated with the non-ideal mixing of the reaction mixture.

## Introduction

Mechanochemistry,[1,2] *i.e.* chemical transformations achieved through the application of mechanical actions, such as grinding, milling, rubbing, shearing, *etc.*, has recently attracted the attention of a wide audience of researchers in organic synthesis and catalysis, the synthesis of and screening for inorganic, metal-organic and pharmaceutical materials and nanoparticle preparation.[3–6] Despite such broad and growing interest, and in contrast to a long history[7] of mechanochemistry and milling in a number of technological areas (mechanical alloying, mineral processing, lubrication),[8] the mechanisms of the mechanochemical reactions have remained largely unknown. Such a lack of mechanistic knowledge is explained by the difficulties associated with monitoring milling reactions, as they take place under the violent impact of hard grinding media, typically

[a]*Ruđer Bošković Institute, Bijenička 54, 10000 Zagreb, Croatia. E-mail: ihalasz@irb.hr; Tel: +38514561184*
[b]*Department of Chemistry and FRQNT Centre for Green Chemistry and Catalysis, McGill University, 801 Sherbrooke St. W., H3A 0B8 Montreal, Canada. E-mail: tomislav.friscic@mcgill.ca; Tel: +5143983959*
[c]*European Synchrotron Radiation Facility (ESRF), Grenoble cedex, France*
[d]*Max-Planck-Institute for Solid State Research, Heisenbergstr.1, 70569 Stuttgart, Germany*

grinding balls of steel, zirconia or tungsten carbide, in a rapidly spinning or oscillating vessel (a grinding jar). The direct monitoring of mechanochemical reactions is further hindered for those mechanochemical reactions that develop rapidly, lasting 30 minutes or less, such as the recently introduced liquid-assisted grinding (LAG) and ion- and liquid-assisted grinding (ILAG) reactions,[2] in which the synthesis of organic or metal-organic products is accelerated and directed by a catalytic amount of a liquid phase, or a combination of a liquid phase with a catalytic ionic additive, respectively. Recently, we have presented the first technique for the real-time and *in situ* observation of mechanochemical transformations by powder X-ray diffraction (PXRD).[9] This methodology is enabled by the use of highly penetrating synchrotron X-rays ($\lambda = 0.14$ Å) and has provided the first direct insight into the mechanochemical formation of metal–organic frameworks known as zeolitic imidazolate frameworks (ZIFs),[9,10] and of pharmaceutical cocrystals.[11] The mechanistic information, however, was mostly qualitative due to difficulties associated with the non-uniform time-dependent distribution of the sample throughout the milling jar, the inability to evaluate the amount of amorphous, non-diffracting material and the inability to quantitatively estimate the X-ray scattering behavior of porous frameworks containing highly mobile and chemically diverse guests.

Herein, using as model reactions the LAG and ILAG milling transformation of zinc oxide and imidazole (**HIm**)† into a non-porous ZIF structure (Fig. 1), we present the results of the first attempt to resolve the above mentioned limitations and achieve quantitative, real-time and *in situ* X-ray diffraction monitoring of mechanochemical reactions, including the assessment of the amorphous content, by adding crystalline silicon to the reaction mixture as an inert internal scattering standard.

## Recent *ex situ* mechanistic studies of mechanochemical milling reactions

Mechanistic studies of mechanochemical reactions have recently been reviewed.[12,13] Most mechanistic studies of milling reactions rely on step-by-step analysis,[14] *i.e.* on the *ex situ* characterization of samples extracted from the mechanochemical reaction mixtures at different milling times. Over the past decade, such studies revealed the unexpectedly dynamic nature of the mechanochemical reactions of organic or metal–organic solids, involving either metastable amorphous phases or quickly interconverting intermediate crystalline phases. The fact that mechanochemical milling can lead to amorphization is well known in the context of inorganic solids, where the amorphous phase may be relatively long-lived.[15] In contrast, the detection and quantification of the metastable amorphous phases in the mechanochemical transformations of "softer" organic and metal-organic substances is highly challenging.[16] Indeed, the importance of the amorphous content in the mechanochemical cocrystallization of organic solids began to be evaluated only recently, for example by a combined use of PXRD and terahertz spectroscopy or by *ex situ* investigation of samples prepared by milling at liquid nitrogen temperatures (cryomilling).[17,18] However, none of the performed studies provided any knowledge of the amorphous phase

† The reaction of ZnO and imidazole was first reported by manual grinding, see: J. Fernández-Bertrán, L. Castellanos-Serra, H. Yee-Madeira and E. Reguera, *J. Solid State Chem.* 1999, **147**, 561.

 

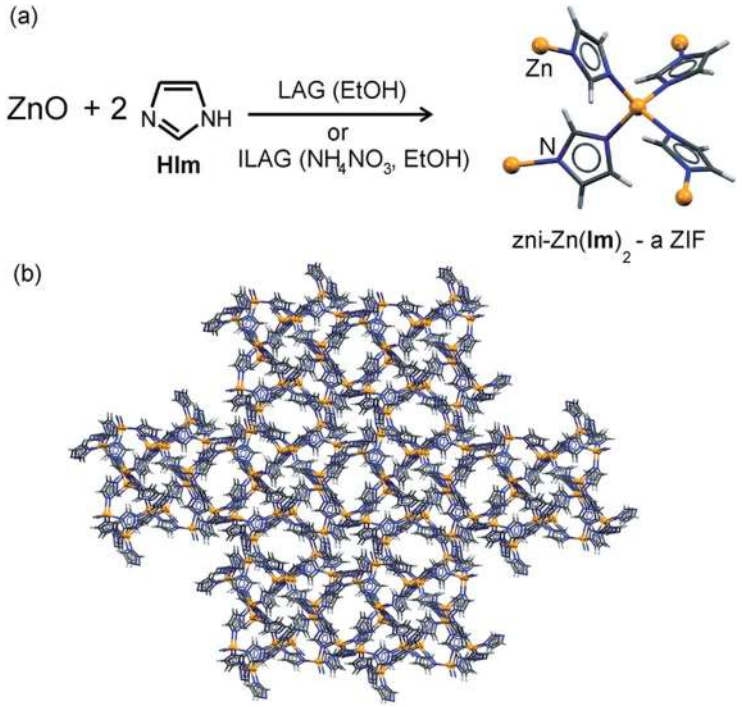


Fig. 1 (a) A schematic representation of the herein studied mechanochemical reaction using either liquid-assisted grinding (LAG) with ethanol (EtOH) or ion- and liquid-assisted grinding (ILAG) with EtOH and the ionic additive $NH_4NO_3$. (b) A view of the reaction product, a non-porous ZIF with a *zni*-topology, viewed down the crystallographic *c*-axis.

content and its structural evolution while the reaction mixture is being milled. Also, due to the metastable nature of the amorphous organic materials and their general sensitivity to moisture and temperature, reliable *ex situ* analyses of amorphous intermediates are difficult to achieve.

Several recent systematic studies have suggested tentative explanations for the appearance of intermediate crystalline phases in mechanochemical reactions, specifically the competition of supramolecular synthons,[19,20] or mass action effects in the early stages of liquid-assisted grinding reactions.[21,22] However, while revealing a dynamic nature for mechanochemical reactions, such studies also made it clear that *ex situ* step-by-step reaction monitoring is too limited for a complete understanding of the mechanochemical processes, requiring the detection and, ideally, the quantification of the short-lived crystalline and amorphous intermediate phases. Such intermediates are likely to have a highly fleeting nature, lasting only seconds or minutes, and their detection and quantification are not compatible with the delays often required for the sample preparation in step-by-step *ex situ* diffraction or spectroscopic analyses. Furthermore, *ex situ* analysis is also inadequate for systems in which sample extraction causes an evaporative loss of a liquid phase, or reactions sensitive to air moisture or $CO_2$.[23,24] Finally, it was also demonstrated that dividing a mechanochemical reaction into segments, including the opening of the reaction jar, may lead to a different product as compared to continuous milling.[14b,25] Thus, the

development of analytical methods capable of monitoring milling reactions without disturbing them is necessary for a proper and reliable understanding of mechanochemistry.

### *In situ* and real-time X-ray diffraction studies of mechanochemical reactions

With the above considerations in mind, we have recently developed[9] the first *in situ* and real-time X-ray diffraction technique for monitoring the course of mechanochemical reactions. This novel and unprecedented methodology[10] is based on the diffraction of high-energy ($E \approx 90$ keV) synchrotron X-rays which are able to penetrate the reaction vessel walls, interact with the sample and again penetrate out of the vessel before being detected on a two-dimensional area detector. Measurements using this technique are also greatly facilitated by replacing the conventional stainless steel reaction vessels with those made of a light-atom, amorphous material such as poly(methyl)methacrylate (PMMA, also known as Perspex or Plexiglas).[9–11] PMMA is a much poorer X-ray scatterer than most metals and gives no diffraction signal. Thus, PMMA milling equipment provides a much more agreeable background for the *in situ* diffraction experiments than the more conventional steel or aluminium alternatives.

This reaction monitoring technique was first used to follow the course of the mechanochemical formation of ZIFs.[9,26] Specifically, the ILAG reaction of ZnO and 2-ethylimidazole (**HEtIm**), which ultimately yields a non-porous close-packed β-quartz (*qtz*) topology zinc(2-ethylimidazolate) framework, was observed to first yield an open framework with zeolite ρ (RHO) topology. Upon further milling this open structure is subsequently replaced by a more dense analcime (ANA) framework (Fig. 2a), which later collapses into the final *qtz*-topology product. As the framework density, and therefore thermodynamic stability,[27] increases in the observed reaction sequence RHO → ANA → *qtz*, this stepwise transformation clearly follows the Ostwald's rule of stages,[28] in which a thermodynamically less stable system (*e.g.* the reactant mixture) converts to the stable one (the ultimate close-packed product) *via* a series of intermediate steps (open frameworks).

The *in situ* and real-time diffraction monitoring technique was also applied to the mechanochemical formation of model pharmaceutical cocrystals.[11] In particular, the group of Rodríguez-Hornedo was the first to propose, on the basis of *ex situ* analysis of samples prepared by cryomilling, that mechanochemical cocrystallisation of carbamazepine and saccharin proceeds *via* an amorphous phase.[18] The application of *in situ* and real-time diffraction monitoring enabled this amorphization to be confirmed[11] by directly observing the gradual loss of the scattering signal of the reaction mixture upon milling (Fig. 2b).

Although the above described proof-of-principle studies provided new and previously inaccessible insights into the mechanisms of the mechanochemical formation of MOFs and cocrystals, this initial monitoring methodology suffered from two significant shortcomings. These are the significant artefactual variation in the intensity of the diffraction signal, which results from the non-uniform distribution of the sample throughout the milling jar, and the inability to quantitatively measure the reaction mixture composition, which prevented the assessment of the amorphous content during milling.

We now demonstrate how our initial *in situ* and real-time monitoring technique can be modified by the addition of a known amount of crystalline silicon as

 

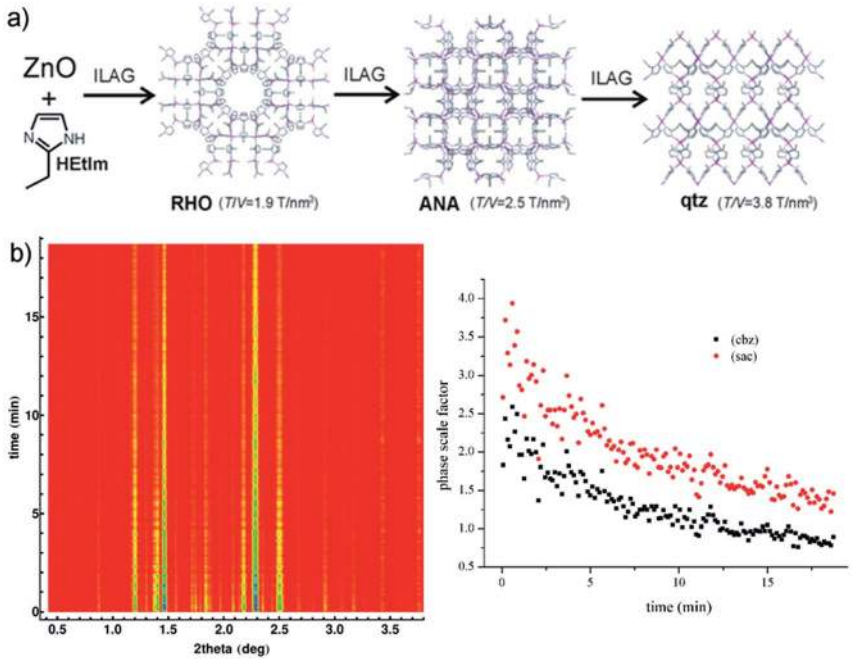


Fig. 2 a) The ILAG synthesis of a zinc(2-ethylimidazolate) ZIF from 2-ethylimidazole and ZnO proceeds through a series of intermediates with decreasing porosity (expressed as *T*/*V*, ratio of tetrahedral centers per unit volume). This stepwise mechanism, observed by *in situ* and real-time X-ray diffraction monitoring, is consistent with the stepwise formation of phases with increasing thermodynamic stability. The formation of the final, close-packed product with α-quartz topology involves the expulsion of the liquid phase from the pores of the zeolite ρ (RHO) and analcime (ANA) intermediates. b) The mechanochemical amorphisation of a mixture of saccharin (sac) and carbamazepine (cbz) during neat milling. Amorphisation is evidenced by the gradual decrease of the diffraction signal from both components (left) and illustrated by the decrease in the phase scale factors extracted from Rietveld refinements (right). The slight random deviations in the scale factor evolution are due to differing amounts of the sample in the X-ray beam in consecutive powder diffraction patterns.

a non-reactive internal X-ray diffraction standard into the reaction mixture. This internal standard technique enabled us to conduct quantitative reaction monitoring, evaluate the reproducibility of mechanochemical reaction kinetics, address the problem of non-uniform distribution of the sample in the reaction jar and, most importantly, establish the extent of the amorphisation of the reaction mixture during mechanochemical milling.

## Materials and methods

The details of the sample preparation, measurement and data processing for the *in situ* and real time diffraction monitoring technique have been reported previously[10] and will be only briefly addressed here. The reaction mixtures were prepared for milling by placing the solid reactants in one half of the reaction vessel, while the liquids and ionic additives were placed in the other along with

one stainless steel ball of 7 mm in diameter (ball mass ≈1.3 g). By careful operation it is possible to join the two halves of the reaction vessel without bringing their contents to contact before milling was initiated. The LAG and ILAG reactions are conveniently described through the $\eta$ parameter, defined as;

$$\eta = \frac{V}{m} \quad (1)$$

where $V$ is the volume of the liquid additive (in microliters) and $m$ is the mass of solid reactants (in milligrams). The use of the $\eta$ parameter allows the direct comparison of neat (dry, $\eta = 0$ μL mg$^{-1}$) and liquid-assisted ($\eta$ range 0–1 μL mg$^{-1}$) mechanochemical reactions to more conventional solvent-based reaction systems, such as slurries ($\eta$ range 2–12 μL mg$^{-1}$) and reactions in solution ($\eta$ > 12 μL mg$^{-1}$). For the herein investigated LAG and ILAG reactions the $\eta$ value was 0.35 μL mg$^{-1}$.

Milling was performed using an in-house modified Retsch MM200 ball mill, which was operated at 30 Hz. The mill was positioned such that a high-energy X-ray beam ($\lambda = 0.14202$ Å, beam size of 300 μm$^2$) generated at the ESRF beamline station ID15B could pass through the vessel oscillating at typically 30 Hz and interact with the sample before being detected on a two-dimensional Pixium charge-coupled detector. The use of an area detector is essential for providing the time resolution in seconds, as it allows the collection of the entire diffraction pattern at once. This, however, comes at an expense of the resolution of integrated diffraction patterns since there are no X-ray optics in the path of the diffracted beam. Each diffractogram was typically obtained by summing 10 frames, each collected with an exposure time of 0.4 seconds. Consecutive diffractograms were typically separated by 9 seconds.

The integration of the raw two-dimensional diffraction patterns was performed using the program Fit2d.[29] Rietveld analysis was performed using the program Topas.[30] The amorphous vessels give rise to two broad peaks which were modelled using the "Peaks phase" of Topas. Further modelling of the background was achieved by a shifted Chebyshev polynomial. The structure models for the crystalline phases were taken from the Cambridge Structure Database (CSD)[31] or the Inorganic Crystal Structure Database (ICSD)[32] and, except for their unit cell parameters, were not refined. The peak shape for each phase was described independently using the Voigt function, taking into account the particle size broadening. The instrumental contribution to peak broadening was estimated by measuring the pattern of corundum measured from a blank milling experiment involving only two corundum balls in an otherwise empty jar.

Since each time-resolved diffraction experiment typically provides several hundreds of individual diffraction patterns, automatic Rietveld refinement greatly facilitates data treatment (Fig. 3). This was achieved by using the command-line version of the program Topas,[30] using the same initial input file for each diffraction pattern. The starting parameter values (unit cell, particle size, scale factor) for specific phases were determined from patterns where this particular phase had a clear diffraction signal. The weight fractions, scale factors or other variable characteristics for a specific diffractogram were conveniently output to a textual file suitable for further analysis and data plotting. Further details of the data treatment have been described previously.[9,10]

The weight fractions for all of the crystalline components with fully known crystal structures can be assessed from a Rietveld refinement. Should there be an

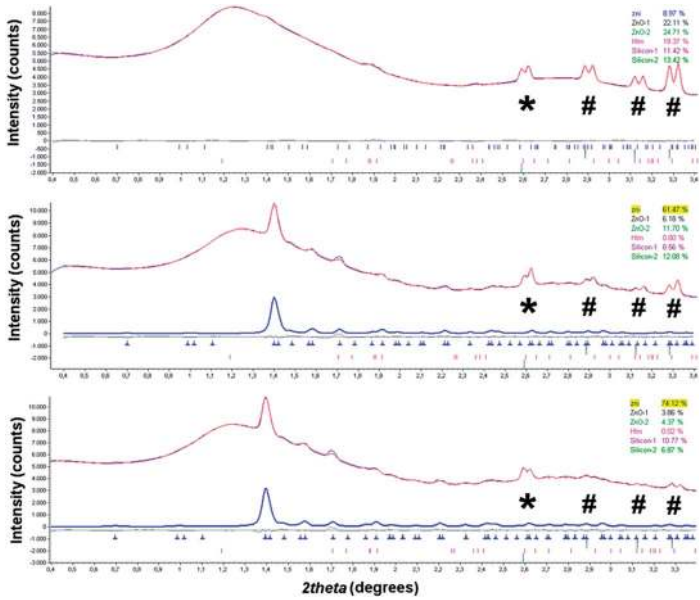


Fig. 3 Example Rietveld refinements of the *in situ* collected diffraction patterns: (top) 10 seconds into the reaction; (middle) 1 minute into the reaction and (bottom) 3 minutes into the reaction. The silicon signal is designated by (*), while (#) designates the ZnO signal. Both are split due to diffraction from the mixture adhering to the two reaction jar walls and were modelled as two phases with the same unit cell, but one having an added refineable shift proportional to tan($\theta$). Since the material is being continuously redistributed throughout the vessel, the relative intensities of the split peaks vary. The contribution of the zni-topology ZIF is shown with a thick blue line below the experimental patterns in the middle and bottom panels. The weight fraction of silicon in the mixture is 14.3%.

amorphous phase present in the mixture, the Rietveld-refined weight fractions of the crystalline components will be overestimated (Fig. 4) by the same factor each. This factor can be estimated by adding a known mass of a highly crystalline and chemically inert standard, which is assumed to retain its crystallinity during milling (in this case silicon). The factor by which the silicon weight fraction is overestimated is the same for all other crystalline components and they all need to be scaled down. After an appropriate scaling and summation of the scaled weight fractions, the difference to a 100% is attributed to the weight fraction of the amorphous phase.

This procedure is applicable if the full crystal structures of all crystalline components are known. This is not the case for a porous material which can accommodate guest species in its pores. Even though the structure of the framework may be well known, the details of the guest species occupying the pores are still an unresolved structural issue. Porous materials thus cannot be included for the calculation of weight fractions using the formula:

$$w_j = \frac{S_j\,(M\ V)_j}{\sum_i S_i\,(M\ V)_i} \tag{2}$$

where $M$ is the molecular mass of the unit cell, $V$ is the unit cell volume, $S$ is the Rietveld-refined scale factor for the particular phase and the sum in the

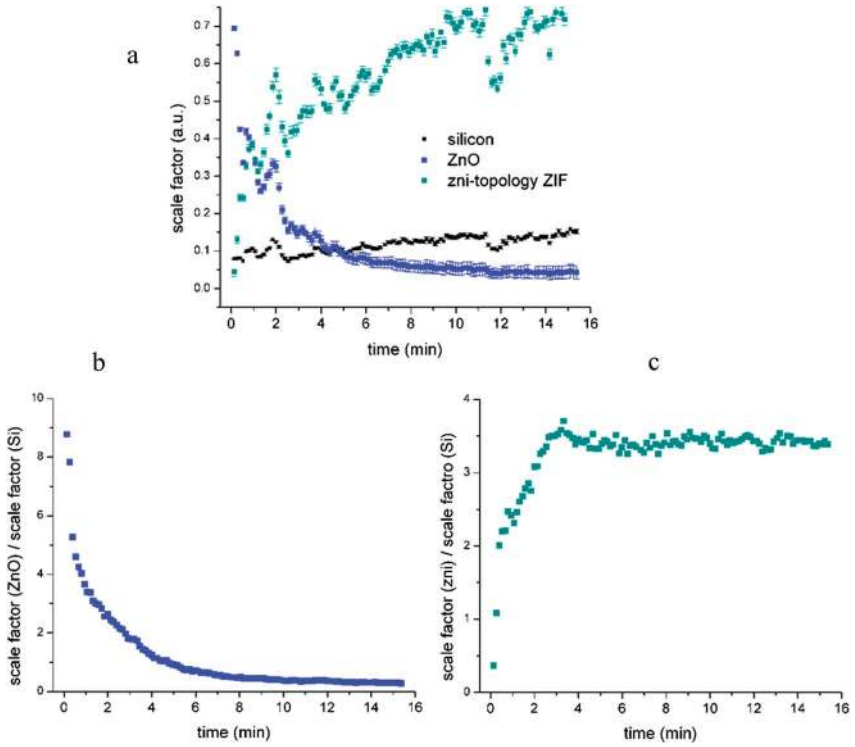


Fig. 4 (a) Scale factors of the internal standard silicon, reactant ZnO and the product zni-Zn(**Im**)$_2$, extracted from time-resolved diffraction patterns (see Fig. 5, top) collected during a LAG (using ethanol as the liquid additive) reaction. The scale factors are affected by the variation of the amount of sample exposed to the X-ray beam during the collection of one diffractogram. The scale factors of (b) ZnO and (c) zni-Zn(**Im**)$_2$ divided by the scale factor of the silicon standard. These plots show that the strength of the diffraction signal may be scaled by that of the silicon signal to reduce the effects of the non-uniform sample distribution and indicate the homogeneity of the mixtures.

denominator runs over all crystalline phases.[33] Porous materials cannot be included since $M_i$ is not known due to the undetermined composition of the pores.

A quantitative analysis requires a reaction mixture to be homogeneous, *i.e.* the sample exposed to the beam for collecting a specific X-ray diffraction pattern must be representative of the entire reaction mixture. Plotting the phase scale factors against time reveals random variations which are a consequence of varying the amount of the sample in the beam during the 4 seconds exposition in the X-ray beam of 300 $\mu m^2$ in size (Fig 4a). However, if the individual phase scale factors are first divided by the scale factor of silicon, the plots become smooth and monotonous and decrease (for ZnO, Fig 4b) and increase (for the zni-topology ZIF, Fig 4c) with time. Thus, the representative diffraction signal intensity for each component may be obtained by scaling with the intensity of the diffraction signal of silicon. The success of this scaling procedure also indicates that the reaction mixture is homogenous.

 

The refined scale factors allow the representative weight fractions of the mixture components to be calculated and, as the time-dependent evolution of the thus calculated weight fractions shows no large oscillations, we conclude that the problem of a non-uniform sample distribution can be overcome by using an internal scattering standard (*i.e.* silicon). Nevertheless, mixture inhomogeneity is still likely to occur at the very beginning of milling. Our findings indicate that the homogeneity of the reaction mixture is most likely achieved within the first 10–20 seconds of milling at 30 Hz (Fig. 4). However, to minimize the effect of the mixture inhomogeneity, the data collected in the first 30 seconds of milling have been excluded from the kinetic analyses.

# Results and discussion

### Quantification of the reaction mixture and reaction kinetics

In order to facilitate the use of Rietveld refinement for the quantitative *in situ* and real-time analysis of a mechanochemical reaction we have focused on the mehanochemical synthesis of the low-porosity (close-packed) zinc imidazolate framework with the zni-topology (Fig. 1). Namely, it was previously reported that LAG and ILAG reactions of ZnO and unsubstituted imidazole lead to the formation of the zni-Zn(**Im**)$_2$ framework (CSD refcode IMIDZB01) without any observable crystalline intermediates,[23] as long as the grinding liquid is ethanol. This provides a relatively simple system consisting of at most three crystalline phases: the reactants ZnO and **HIm** and the product framework zni-Zn(**Im**)$_2$. As all of these phases can be considered non-porous, their weight fractions should be readily accessible *via* Rietveld refinement of the *in situ* collected diffractograms. In order to evaluate the reproducibility of the mechanochemical reaction kinetics, we have performed each LAG and ILAG reaction twice.

### Analysis of the ILAG reaction

The time-resolved diffractograms for the two identical ILAG reactions are shown in Fig. 5, along with the associated reaction kinetics curves obtained by Rietveld analysis. The inspection of the time-resolved diffractograms immediately reveals the rapid formation of the zni-Zn(**Im**)$_2$ product, which appears within less than 30 seconds of milling. The time-resolved diffractograms also display considerable variations in the intensity of the diffraction signal of the reaction mixture. These variations, as noted in our first report,[9] are a result of the variation of the amount of sample in the path of the X-ray beam and would normally prevent the quantitative monitoring of the reaction course through Rietveld analysis. In order to circumvent this obstacle, we normalised the X-ray diffraction signals of ZnO, **HIm** and Zn(**Im**)$_2$ using the diffraction signal of silicon (Fig. 4). The effectiveness of such a normalization procedure for eliminating the fluctuations of the diffraction signal is illustrated by plotting against time the weight fractions of ZnO, **HIm** and zni-Zn(**Im**)$_2$ obtained by quantitative Rietveld analysis (Fig. 5). The resulting kinetic plots reveal a largely smooth increase in the content of the zni-Zn(**Im**)$_2$ product, and similarly smooth decreases in the content of reactants ZnO and **HIm**.

Even though the time-dependent composition of the reaction mixture is fairly similar (within *ca.* 5 weight%) for the two ILAG reactions, the shapes of the curves

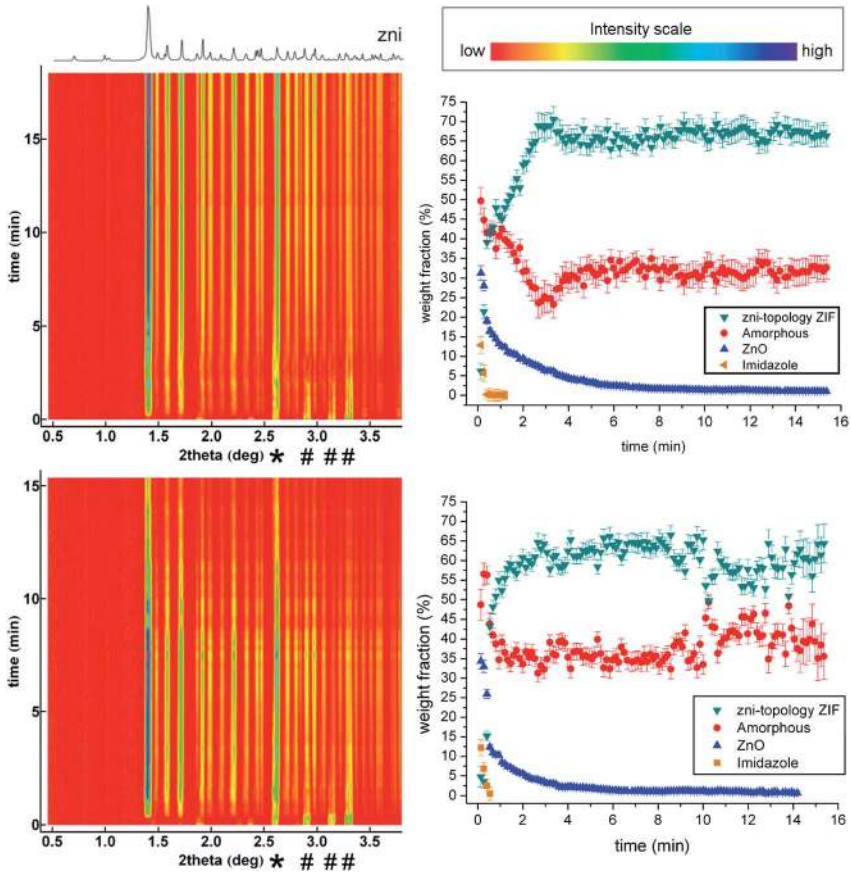


Fig. 5 The time-resolved diffractograms (on the left) and Rietveld-extracted weight fractions (on the right) of the two times repeated ILAG reaction of ZnO (160 mg) and HIm (272 mg) using ethanol (150 μL) as the grinding liquid and ammonium nitrate (18 mg) as the ionic additive. On the left are the time-resolved difractograms, on the right are the Rietveld-extracted weight fractions. The calculated PXRD pattern of the zni-topology ZIF and the colour code for the time resolved diffractogram are given at the top of the figure. The asterisks (*) designate the silicon signal while the hash sign (#) designates the ZnO signal. The weight fractions have been recalculated as if there was no silicon in the reaction mixture.

representing ZIF formation in two experiments are different. In one experiment the ZIF forms at an apparently constant rate, following an initial rapid rise in its weight fraction. In the other, ZIF formation follows a more common sigmoidal curve.[9] We note that this may be due to non-ideal mixing and the distribution of the reaction mixture throughout the jar at the very start of milling. Such effects are particularly likely in LAG and ILAG reactions where the reaction mixture might be sticky and adhere to the reaction vessel walls. In such cases the measured weight fractions and reaction kinetics are influenced not only by the chemical reaction taking place in the free-flowing powder but also by the removal of material adhering to the reaction vessel walls.

The time-resolved diffractograms reveal the rapid and complete disappearance of the diffraction signal of crystalline **HIm** within 30 seconds, after which this

 

phase (CSD code IMAZOL14) was excluded from the Rietveld analysis. The rapid loss of crystalline **HIm** is assigned to several parallel processes, including the dissolution in the grinding liquid and amorphization, as well as the chemical reaction with the salt additive and with ZnO. The formation of zni-Zn(**Im**)$_2$, in agreement with our earlier qualitative study, is rapid and reaches full extent within *ca.* 4 minutes for the two identically prepared ILAG reactions.

The Rietveld analysis allowed us to quantitatively evaluate, for the first time, the amount of the amorphous phase present in a mechanochemical reaction while it is being milled. The sum of the weight fractions of the crystalline reactants and products in the reaction mixture dropped very quickly (within a minute) from the initial 100% to a relatively constant value of 60–65%, indicating that, during milling, as much as *ca.* 35–40% of the reaction mixture weight is present in an amorphous form. Previous *ex situ* investigations of the mechanochemical reactivity established that neat grinding reactions can involve *ca.* 25–35% of the reaction mixture in an amorphous form.[17] Analogous liquid-assisted reactions always gave a fully crystalline (100%) product and were too fast to allow the evaluation of the amorphous content by *ex situ* studies. Thus, the herein described quantitative Rietveld analysis is the first clear demonstration that the amorphous phase can be relevant in a liquid-assisted mechanochemical reaction. This result is consistent with the work of Yuan *et al.*, who proposed that the mechanochemical transformations of different MOF topologies might be assisted by amorphization during LAG.[35] The kinetic plots show that, after *ca.* 4 min milling, the weight fraction of the crystalline zni-Zn(**Im**)$_2$ remains relatively constant whereas ZnO is still being depleted (Fig. 5). This observation suggests the direct transformation of crystalline ZnO into an amorphous ZIF.

As noted in the introduction, the disappearance of the diffraction signal of crystalline **HIm** from the time-resolved diffractograms is a result of several physical and chemical processes and cannot be used for quantitative monitoring of the reaction kinetics. Similarly, the formation of crystalline zni-Zn(**Im**)$_2$ involves at least three processes: the reaction of ZnO with **HIm**, the nucleation of the ZIF and its growth. Consequently, neither **HIm** nor zni-Zn(**Im**)$_2$ is a suitable target for the quantitative diffraction monitoring of the chemical reaction between ZnO and **HIm**. In contrast, the disappearance of the diffraction signal of the harder inorganic substance ZnO is expected to be less affected by the amorphization under the employed milling conditions, offering an opportunity to evaluate the reaction kinetics. Recently, Ma and co-workers have used Raman spectroscopy to monitor *ex situ* the fraction of unreacted **HIm** at different stages of the mechanochemical reaction of ZnO and **HIm** in the presence of DMF.[34] These measurements revealed "pseudo-fluid" behaviour in which the kinetics of disappearance of **HIm** resembled a 2$^{nd}$-order solution reaction. Here, the non-linear fitting of the time-dependent weight fraction of ZnO (Fig. 6a,b) revealed an excellent fit to the 1$^{st}$ order reaction model. Attempts of non-linear fitting to the 2$^{nd}$ order reaction kinetics gave poorer results (Fig. 6c,d). In both cases the fitting was performed without taking into account the data acquired during the first 30 seconds of milling, due to non-ideal mixing at the very onset of milling. Another reason to ignore those data is because the consumption of ZnO at the onset of milling is likely to be strongly affected by the surface and particulate properties of the commercial ZnO reagent. Although the two identically performed ILAG experiments exhibited an excellent fit to 1$^{st}$ order reaction kinetics, the two

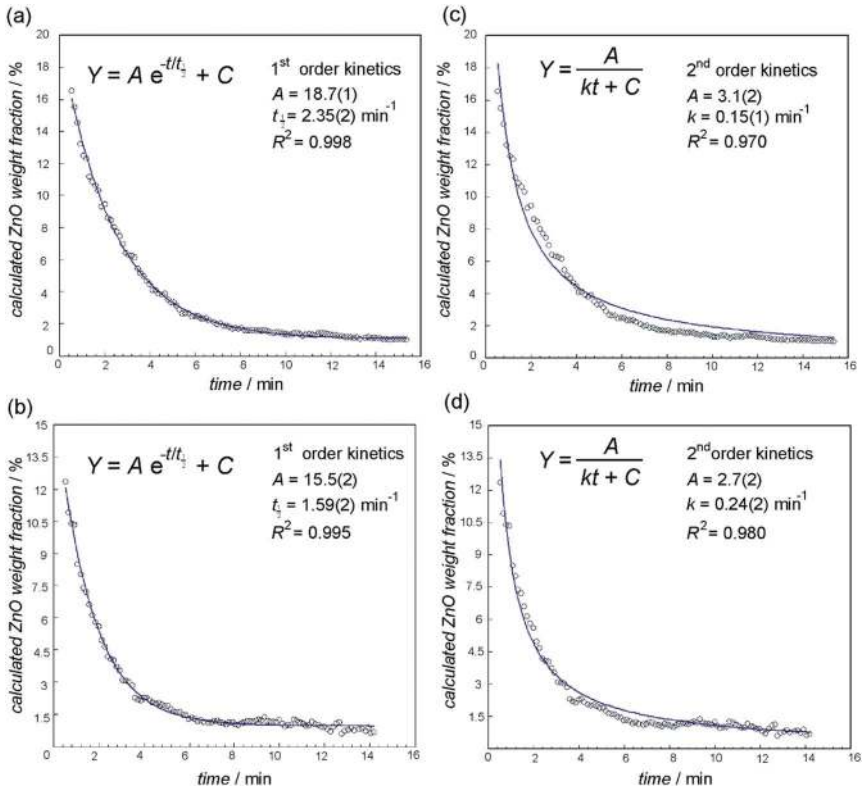


Fig. 6 The non-linear fitting of the time-dependent weight fraction of ZnO, obtained by automated Rietveld refinement of time-resolved diffraction data, to solution-like reaction kinetics laws. The data for the two identically prepared ILAG reactions in (a) and (b) display a superior fit to first-order reaction kinetics. The same two sets of data give a visually and numerically poorer fit to second-order kinetics in (c) and (d). For all fitting procedures the data from the first 30 seconds of milling were excluded, in order to minimise the effects of mixture inhomogeneity and of the initial reactant sample texture.

experiments yielded considerably different values of kinetic parameters (Fig. 6) for ZnO consumption, thus indicating the complexity of the mechanochemical processes being studied. Whereas the possibility that the mechanochemical reaction follows 1st order reaction kinetics conflicts the *ex situ* spectroscopic work,[34] we note there are also significant differences between the currently and previously studied systems. The previously studied reaction involved a significantly smaller content of liquid ($\eta = 0.05$ μL mg$^{-1}$), suggesting a lower level of molecular mobility compared to the herein explored systems ($\eta = 0.35$ μL mg$^{-1}$). Presumably, the higher liquid content in the current study could facilitate contact between ZnO and **HIm**, which was identified as the rate-determining process in previous work. Thus, with a higher liquid content the mechanochemical reaction might be controlled by a different process, such as the rate of activation of ZnO by amorphisation or dissolution, therefore leading to reaction kinetics resembling a 1st order rate law. However, such interpretations remain highly speculative due to a significant oversimplification of the mechanochemical reactivity of ZnO which not only consists of several events, including amorphisation, dissolution and

particle comminution, but also requires efficient product removal‡ to ensure the exposure of fresh reactant surface. Finally, it is also important to keep in mind that Raman spectroscopy and PXRD are complementary methods, as the former provides largely information about a thin layer of the sample, whereas the latter provides insight into the sample bulk.

### Analysis of the LAG reaction

Compared to the analogous ILAG reactions, the two identically prepared LAG reactions (Fig. 7) proceeded more slowly, which is consistent with the previous observation[2b,9] that salt additives improve the mechanochemical reactions of metal oxides.

The comparison of the Rietveld analyses for the ILAG and LAG reactions reveals that $NH_4NO_3$ accelerated not only the ZIF formation, but also the disappearance of the reactant **HIm**. This is consistent with a previously proposed reaction model in which the catalytic activity of the ammonium salts involves the activation of the imidazole ligand by protonation.[36] In particular, it took over 1 minute for the diffraction signals of **HIm** to disappear from the PXRD patterns of the LAG reaction mixture. The appearance of crystalline zni-Zn(**Im**)$_2$ was sufficiently slow to exhibit sigmoidal growth behaviour, which is characteristic for processes involving nucleation and crystal growth from an amorphous phase.[9,37] Rietveld analysis reveals that a significant fraction (*ca.* 35% by weight) of the LAG reaction is amorphous during milling. Whereas the content of ZnO in the ILAG reactions decreases steadily by milling and almost completely disappears in less than 10 minutes, in the LAG reaction the weight fraction of ZnO was found to drop to ~15% (*ca.* one-third of its initial value) within *ca.* 4 minutes and after that remained fairly constant. Consequently, it is reasonable to assume that the LAG reaction reaches its maximum extent within 5 minutes.‡ Kinetic analyses were, therefore, conducted only on the data collected within that timeframe. In this case, attempts to analyse the reaction course through non-linear fitting of the data to solution-type kinetic rate laws clearly indicated that the reaction progress is best described by 1$^{st}$ order reaction kinetics (Fig. 8).

### Prospects of amorphous phase characterisation *via* pair distribution function and its time evolution

The *in situ* X-ray diffraction technique offers another possibility which we wish to discuss. Namely, the amorphous phase, which is abundantly present in the herein studied mechanochemical transformation, gives no diffraction signal but does have a scattering contribution which was thus far neglected. It seems reasonable to assume that the short-range order in the amorphous phase will have an influence on the nucleation and crystal growth of the bulk crystalline species. Therefore, it seems imperative to develop a means to obtain structural

‡ A recent transmission electron microscopy study of the dry grinding reaction of ZnO and 2-methylimidazole to form the popular framework ZIF-8 revealed the entrapment of the zinc oxide particles within a shell of the ZIF product, hindering the advance of the reaction. The apparently poor advance of the LAG reaction might be tentatively explained by a similar entrapment of ZnO reactant particles within a shell of the product zni-Zn(**Im**)$_2$. As the framework zni-Zn(**Im**)$_2$ is non-porous, it could be efficient in preventing a further mechanochemical reaction of ZnO. See: S. Tanaka, K. Kida, T. Nagaoka, T. Ota and Y. Miyake, *Chem. Commun.* 2013, **49**, 7884.

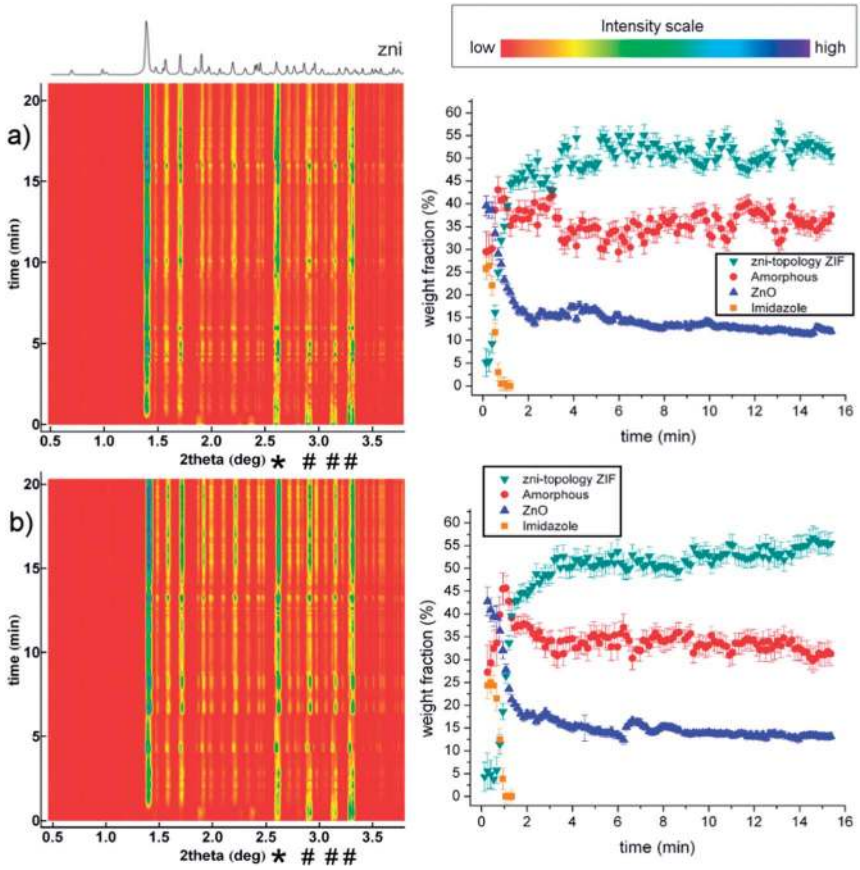


Fig. 7 (a) and (b) Time-resolved diffractograms (left) and weight fractions of the crystalline and amorphous reaction components extracted by Rietveld refinement (right) for two identically prepared LAG reactions of ZnO (160 mg, 2 mmol) and **HIm** (272 mg, 4 mmol) using ethanol (150 μL, 2.6 mmol, $\eta = 0.35$ μL mg$^{-1}$) as the grinding liquid. The calculated PXRD pattern of the reaction product zni-topology Zn(**Im**)$_2$ framework and the colour scheme for the time-resolved diffractogram are given at the top of the figure. The time-dependent variations in the intensity of the diffraction signal of the reaction mixture are related to differing amounts of the sample in the beam and illustrate well the need for an internal diffraction standard. The asterisks (*) designate the silicon signal while the hash sign (#) designates the ZnO signal. The weight fractions have been recalculated as if there was no silicon in the reaction mixture. The weight fraction of ZnO rises slightly between 6 and 9 minutes which is correlated with the stronger diffraction signal of the whole reaction mixture. This indicates that the standard deviations of the weight fractions as determined from the Rietveld refinement are underestimated.

information of the amorphous intermediate and determine if it is changing during milling. The X-ray scattering technique suitable for such analysis is the pair distribution function (PDF). High-energy X-rays available at ID15B are well suited to collect scattering data to high Q values as needed for reliable PDF determination. In such an experiment the background contribution of the moving amorphous reaction jar would need to be carefully subtracted in order to leave only the sample's scattering contribution in the pattern. Should this be

 

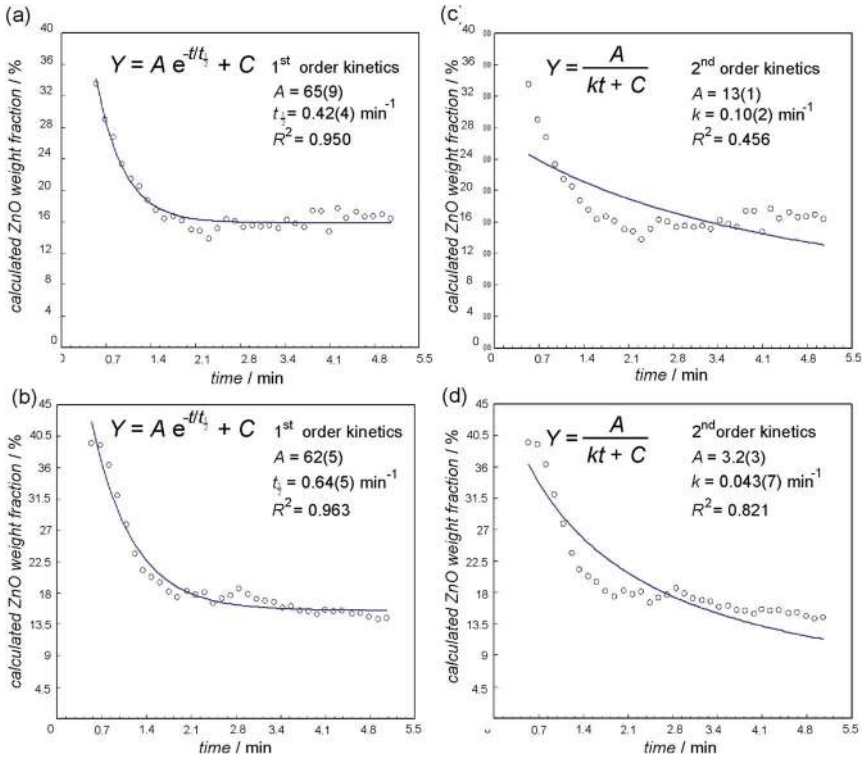


Fig. 8 The non-linear fitting of the time-dependent weight fraction of ZnO, obtained by automated Rietveld refinement of the time-resolved diffraction data, to solution-like reaction kinetics laws. The data for the two identically prepared LAG reactions in (a) and (b) display a superior fit to first-order reaction kinetics as compared to second-order reaction kinetics. The same two sets of data give a visually and numerically poorer fit to second-order kinetics in (c) and (d). For all fitting procedures the data from the first 30 seconds of milling were excluded, in order to minimise the effects of mixture inhomogeneity, and of the initial reactant sample texture.

possible, the possibility to structurally characterise the amorphous phase and its time evolution would arise, allowing for an even deeper insight into the mechanochemical reaction course. These experiments will be the subject of our further studies using the real-time and *in situ* X-ray scattering technique. The current experimental setup should require only one modification, the detector would need to be placed closer to the reaction jar to be able to collect scattering data to higher Q values.

### Difficulties due to the presence of a liquid phase

As our next target we wanted to address the reproducibility of the reaction kinetics for a more complex mechanochemical transformation, the reaction of ZnO and 2-ethylimidazole (**HEtIm**) which proceeds *via* open structures with RHO and ANA topologies to form a close-packed qtz-topology ZIF as the final product (Fig. 2a). The corresponding time-resolved diffractograms (Fig. 9) for the LAG reaction conducted at $\eta = 0.08\ \mu L\ mg^{-1}$ demonstrate a noticeable difference between these

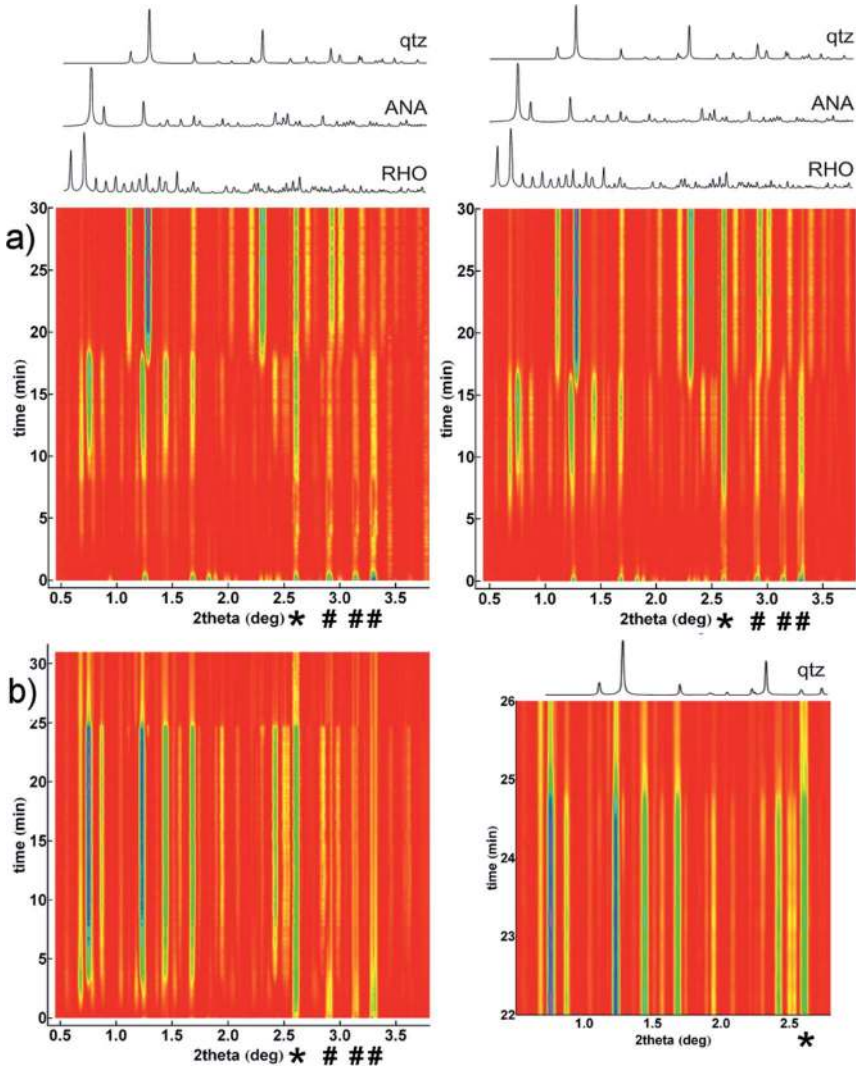


Fig. 9 a) The time-resolved difractograms of the two times repeated mechanochemical ILAG synthesis of porous ZIFs based on 2-ethylimidazole with silicon present ($w$(Si) = 12%, $V$(DMF) = 50 μL, $\eta$ = 0.08 μL mg$^{-1}$). b) The time-resolved diffractogram of the above ILAG reaction using more liquid ($V$(DMF) = 150 μL, $\eta$ = 0.23 μL mg$^{-1}$) and its zoomed part emphasising the appearance of a weak signal of the qtz-topology product. The calculated diffraction patterns of the ZIFs are given at the top of the figure. The asterisks (*) designate the position of the silicon signal while the hash sign (#) designates the ZnO signal.

two identically prepared reactions, as the reaction products in one of them appear *ca.* 3 minutes earlier. The appearance of the final qtz-topology product also takes place *ca.* 3 minutes earlier in that particular system. The key to this apparent irreproducibility of reaction kinetics lies in the observation that the diffraction signals in both reactions disappear very quickly after the onset of milling. Indeed, the time-resolved diffractogram remains almost completely featureless for almost 5 minutes and 8 minutes in each of the two reaction systems.

 

Whereas this at first resembles the amorphisation of the reaction mixture, the disappearance of features from the diffraction patterns is complete, also including the reflections of the added crystalline silicon standard. The latter is a clear indication that the loss of the diffraction signal is caused by the lack of sample in the X-ray beam, *i.e.* it is due to an extremely non-uniform sample distribution in the jar. Indeed, LAG reaction mixtures are sometimes seen to strongly adhere to either the walls or the ends of the milling jar, and sometimes even form a hard shell around the milling ball. This also provides a suitable rationalisation for the apparent difference in the reaction kinetics between the two reaction systems, as it is reasonable to assume that the reactivity in a milled, free-flowing powder will be different than for a mostly static sample adhering to the milling vessel or ball. Indeed, such an effect has been noted by Michalchuk and co-workers in the milling cocrystallisation of glycine and malonic acid where two distinct reactivity regimes were observed: (i) the shearing of the sample adhering to the jar wall and (2) the compression of the sample adhering to the jar ends.[38] Whereas these effects of liquid-induced non-uniform sample distribution cannot yet be predicted or resolved, we note that the presence of an internal standard in the mixture allows such events to be identified and distinguished from the reaction mechanism and kinetics. This is well illustrated in the ILAG experiment involving ZnO and 2-ethylimidazole at a higher $\eta$ value (0.23 μL mg$^{-1}$). Under such conditions, the abundant liquid additive becomes included as a guest into the open structures of the RHO and ANA intermediates, therefore stabilising them. The stabilisation is evidenced by the persistence of the ANA form up to *ca.* 25 minutes milling (compared to *ca.* 16–19 minutes at $\eta = 0.08$ μL mg$^{-1}$). Eventually, however, the open structure collapses, as evidenced by the appearance of X-ray reflections of the qtz-framework. Within a couple of minutes, however, the features in the time-resolved diffractogram, including the reflection of the silicon standard, rapidly lose in intensity. Rather than amorphisation, an explanation of such behaviour lies in the release of the grinding liquid that was included in the open ANA-intermediate, resulting in a pasty sample that sticks to the grinding jar walls and is, therefore, effectively removed from the path of the X-ray beam.

## Conclusions and outlook

We have demonstrated how the addition of crystalline silicon as an internal X-ray diffraction standard can help circumvent the limitations of the recently introduced technique for *in situ* and real-time reaction monitoring. In particular, the use of an internal standard ameliorated the variation in the diffraction signal intensity caused by the non-uniform distribution of the sample throughout the milling jar and allowed the quantitative analysis of the milled reaction mixtures using the Rietveld method. This allowed, for the first time, the *in situ* detection and evaluation of the amorphous content in a progressing mechanochemical reaction. The results have provided strong evidence that both the liquid-assisted and ion- and liquid-assisted reactions can involve extensive amorphization (up to 35% by weight) of the reaction mixture. As amorphous phases are often proposed as intermediates in mechanochemical processes, we believe that the ability to detect and, indeed, quantify the amorphous content within a milling reaction *in situ* is an important step towards creating an all-encompassing model of mechanochemical reactivity.

## References


1 S. L. James, P. Collier, I. Parkin, G. Hyatt, D. Braga, L. Maini, W. Jones, C. Bçlm, A. Krebs, J. Mack, D. Waddell, W. Shearouse, A. G. Orpen, C. J. Adams, T. Friščić, J. W. Steed and K. D. M. Harris, *Chem. Soc. Rev.*, 2012, **41**, 413.

2 A. V. Trask, W. D. S. Motherwell and W. Jones, *Chem. Commun.*, 2004, 890; T. Friščić, D. G. Reid, I. Halasz, R. S. Stein, R. E. Dinnebier and M. J. Duer, *Angew. Chem., Int. Ed.*, 2010, **49**, 712.

3 V. Šepelák, A. Düvel, M. Wilkening, K.-D. Becker and P. Heitjans, *Chem. Soc. Rev.*, 2013, **42**, 7507–7520.

4 (*a*) T. Friščić, *Chem. Soc. Rev.*, 2012, **41**, 3493; (*b*) A. Lazuen-Garay, A. Pichon and S. L. James, *Chem. Soc. Rev.*, 2007, **36**, 846; (*c*) D. Braga, S. L. Giaffreda, F. Grepioni, A. Pettersen, L. Maini, M. Curzi and M. Polito, *Dalton Trans.*, 2006, 1249; (*d*) T. Friščić, I. Halasz, V. Štrukil, M. Eckert-Maksić and R. E. Dinnebier, *Croat. Chem. Acta*, 2012, **85**, 367.

5 (*a*) D. Braga, L. Maini and F. Grepioni, *Chem. Soc. Rev.*, 2013, **42**, 7638; (*b*) A. Bruckmann, A. Krebs and C. Bolm, *Green Chem.*, 2008, **10**, 1131; (*c*) A. Stolle, T. Szuppa, S. E. S. Leonhardt and B. Ondruschka, *Chem. Soc. Rev.*, 2011, **40**, 2317.

6 P. Baláž, M. Achimovičá, M. Baláž, P. Billik, Z. Cherkezova-Zheleva, J. M. Criado, F. Delogu, E. Dutková, E. Gaffet, F. J. Gotor, R. Kumar, I. Mitov, T. Rojac, M. Senna, A. Streletskii and K. Wieczorek-Ciurowa, *Chem. Soc. Rev.*, 2013, **42**, 7571.

7 (*a*) L. Takacs, *Chem. Soc. Rev.*, 2013, **42**, 7649; (*b*) L. Takacs, *J. Mater. Sci.*, 2004, **39**, 4987.

8 C. Suryanarayana, *Prog. Mater. Sci.*, 2001, **46**, 1.

9 T. Friščić, I. Halasz, P. J. Beldon, A. M. Belenguer, F. Adams, S. A. J. Kimber, V. Honkimäki and R. E. Dinnebier, *Nat. Chem.*, 2013, **5**, 66.

10 I. Halasz, S. A. J. Kimber, P. J. Beldon, A. M. Belenguer, F. Adams, V. Honkimäki, R. C. Nightingale, R. E. Dinnebier and T. Friščić, *Nat. Protoc.*, 2013, **8**, 1718.

11 I. Halasz, A. Puškarić, S. A. J. Kimber, P. J. Beldon, A. M. Belenguer, F. Adams, V. Honkimäki, R. E. Dinnebier, B. Patel, W. Jones, V. Štrukil and T. Friščić, *Angew. Chem., Int. Ed.*, 2013, **52**, 11538.

12 E. Boldyreva, *Chem. Soc. Rev.*, 2013, **42**, 7719.

13 T. Friščić and W. Jones, *Cryst. Growth Des.*, 2009, **9**, 1621.

14 (*a*) M. R. Caira, L. R. Nassimbeni and A. F. Wildervanck, *J. Chem. Soc., Perkin Trans. 2*, 1995, 2213; (*b*) V. Štrukil, L. Fábián, D. G. Reid, M. J. Duer, G. J. Jackson, M. Eckert-Maksić and T. Friščić, *Chem. Commun.*, 2010, **46**, 9191.

15 V. Šepelák, S. Bégin-Colin and G. Le Caër, *Dalton Trans.*, 2012, **41**, 11927.

16 J. F. Willart and M. Descamps, *Mol. Pharmaceutics*, 2008, **5**, 905.

17 K. L. Nguyen, T. Friščić, G. M. Day, L. F. Gladden and W. Jones, *Nat. Mater.*, 2007, **6**, 206.

18 A. Jayasankar, A. Somwangthanaroj, Z. J. Shao and N. Rodríguez-Hornedo, *Pharm. Res.*, 2006, **23**, 2381.

19 D. Cinčić, T. Friščić and W. Jones, *J. Am. Chem. Soc.*, 2008, **130**, 7524–7525.

20 S. Karki, T. Friščić and W. Jones, *CrystEngComm*, 2009, **11**, 470–481.

21 L. Fábián and T. Friščić, *CrystEngComm*, 2009, **11**, 743–745.


 

22 F. C. Strobridge, N. Judaš and T. Friščić, *CrystEngComm*, 2010, **12**, 2409–2412.
23 D. Braga, S. L. Giaffreda, F. Grepioni and M. Polito, *CrystEngComm*, 2004, **6**, 458.
24 G. A. Bowmaker, Effendy, J. V. Hanna, P. C. Healy, S. P. King, C. Pettinari, B. W. Skelton and A. H. White, *Dalton Trans.*, 2011, **40**, 7210.
25 K. Užarević, I. Halasz, I. Đilović, N. Bregović, Mirta Rubčić, D. Matković-Čalogović and V. Tomišić, *Angew. Chem., Int. Ed.*, 2013, **52**, 5504.
26 P. J. Beldon, L. Fábián, R. S. Stein, A. Thirumurugan, A. K. Cheetham and T. Friščić, *Angew. Chem., Int. Ed.*, 2010, **49**, 9640.
27 D. W. Lewis, A. R. Ruiz-Salvador, A. Gomez, L. M. Rodriguez-Albelo, F.-X. Coudert, B. Slater, A. K. Cheetham and C. Mellot-Draznieks, *CrystEngComm*, 2009, **11**, 2272.
28 J. C. Burley, M. J. Duer, R. S. Stein and R. M. Vrcelj, *Eur. J. Pharm. Sci.*, 2007, **31**, 271.
29 A. P. Hammersley, *ESRF Internal Report*, 1997, **ESRF97HA02T**.
30 Topas, version 4.2, Bruker-AXS, Karlsruhe, Germany.
31 Cambridge Structural Database (CSD), v. 5.34 (update Nov 2012).
32 Inorganic Crystal Structure Database, FIZ Karlsruhe, Karlsruhe, Germany.
33 R. J. Hill and C. J. Howard, *J. Appl. Crystallogr.*, 1987, **20**, 467–474.
34 X. Ma, W. Yuan, S. E. J. Bell and S. L. James, *Chem. Commun.*, 2014, **50**, 1585–1587.
35 W. Yuan, T. Friščić, D. Apperley and S. L. James, *Angew. Chem., Int. Ed.*, 2010, **49**, 3916.
36 M. J. Cliffe, C. Mottillo, R. S. Stein, D.-K. Bučar and T. Friščić, *Chem. Sci.*, 2012, **3**, 2495.
37 (*a*) A. Khawam and D. R. Flanagan, *J. Phys. Chem. B*, 2006, **110**, 17315; (*b*) F. L. Cumbrera and F. Sánchez-Bajo, *Thermochim. Acta*, 1995, **266**, 315.
38 A. A. L. Michalchuk, I. A. Tumanov and E. V. Boldyreva, *CrystEngComm*, 2013, **15**, 6403.